The Concept and Analytical Investigation of CO_2 and Steam Co-Electrolysis for Resource Utilization in Space Exploration

Michael G. McKellar[*], Carl M. Stoots[†], Manohar S. Sohal[‡]
Idaho National Laboratory, Idaho Falls, ID, 83415-3710

Lila M. Mulloth[§], Bernadette Luna[¶]
NASA Ames Research Center, Moffett Field, California 94035-1000

and

Morgan B. Abney[**]
NASA Marshall Space Flight Center, Huntsville, Alabama, 35812

CO_2 acquisition and utilization technologies will have a vital role in designing sustainable and affordable life support and *in situ* fuel production architectures for human and robotic exploration of Moon and Mars. For long-term human exploration to be practical, reliable technologies have to be implemented to capture the metabolic CO_2 from the cabin air and chemically reduce it to recover oxygen. Technologies that enable the *in situ* capture and conversion of atmospheric CO_2 to fuel are essential for a viable human mission to Mars. This paper describes the concept and mathematical analysis of a closed-loop life support system based on combined electrolysis of CO_2 and steam (co-electrolysis). Products of the co-electrolysis process include oxygen and syngas (CO and H_2) that are suitable for life support and synthetic fuel production, respectively. The model was developed based on the performance of a co-electrolysis system developed at Idaho National Laboratory (INL). Individual and combined process models of the co-electrolysis and Sabatier, Bosch, Boudouard, and hydrogenation reactions are discussed and their performance analyses in terms of oxygen production and CO_2 utilization are presented.

Nomenclature

ARC = *Ames Research Center*
C = Carbon
CH_4 = *Methane*
CO = Carbon monoxide
CO_2 = *Carbon dioxide*
H_2 = *Hydrogen*
H_2O = *water*
ISS = *International Space Station*
LPCOR = *Low-power CO_2 removal*

---

[*] Research and Development Engineer, Advanced Process and Decision Systems, P.O Box 1625
[†] Senior Research Engineer, Thermal Fluids and Heat Transfer Department
[‡] Senior Research Engineer, Energy Efficiency and Industrial Technology
[§] Senior Engineer, Science Applications International Corporation
[¶] Research Scientist, NASA Ames Research Center
[**] Aerospace Engineer, Environmental Control and Life Support Systems

O_2 = *Oxygen*
RWGS = *Reverse water gas shift*
SOFC = *Solid Oxide Fuel Cell*
SOEC = *Solid Oxide Electrolysis Cell*
TRL = *Technology Readiness Level*

I. Introduction

Removal of metabolic CO_2 from breathing air is a fundamental requirement for life support in a manned spaceflight. As the duration of the flight and the distance from earth increase, the need for recovering oxygen from the waste CO_2 become imperative. Closed-loop life support warrants recovery and recycling of consumables from metabolic byproducts through air, water, and solid waste treatment processes. Chemical reduction technologies for CO_2 are critical for establishing closed-loop atmosphere (air) revitalization systems in space missions beyond low-earth orbit. NASA's is also interested in CO_2 reduction technologies for *in situ* fuel production on Mars.

The major processes of a typical closed-loop air revitalization architecture for space cabin include CO_2 removal, CO_2 recovery, CO_2 (chemical) reduction, and oxygen generation through water electrolysis.

A low-power CO_2 removal (LPCOR) system is being developed at NASA Ames Research Center[1] (ARC) to perform the CO_2 removal and recovery functions. The primary objective of the study presented in this paper is to investigate the synergy between LPCOR and the CO_2 and steam co-electrolysis process that was developed at the Idaho National Laboratory (INL). The model was developed based on the experimental data obtained using the co-electrolysis system developed at INL, sized to process 1 kg CO_2 per day (one-person equivalent). Application of the co-electrolysis in NASA's life support system has been analyzed as an independent technology and also in combination with other key CO_2 reduction technologies. NASA has considered a number CO_2 reduction options. Among them, the Sabatier and Bosch processes have gained considerable attention and development.[2] NASA's current baseline air revitalization plan for the International Space Station (ISS), for example, is based on the Sabatier CO_2 reduction technology. NASA has also investigated CO_2 (only) electrolysis and the co-electrolysis processes to a limited extent in the past.

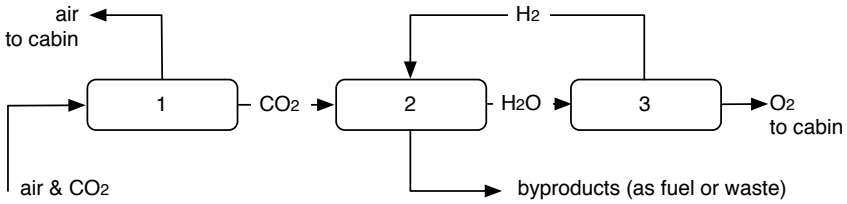

Figure 1. Schematic of a typical closed-loop air revitalization system. (1) CO_2 removal and recovery system, (2) CO_2 chemical reduction system, (3) water electrolysis system.

Sabatier technology is the most advanced in terms of its technology readiness level (TRL). Equation (1) represents the Sabatier reaction.

$$CO_2 + 4H_2 \rightarrow 2H_2O + CH_4 \quad (1)$$

The stoichiometry suggests that all of the oxygen in CO_2 can be recovered as water at a hydrogen to CO_2 molar ratio of 4:1. In practice, however, the Sabatier development unit is operated using a 3.5:1 hydrogen to CO_2 molar ratio that constitutes 14% excess CO_2.[3] Water is separated from methane and is electrolyzed in the water electrolysis system, as shown in Figure 1, to produce O_2 and H_2. The methane has to be separated from the excess CO_2 if it is to be stored or used as fuel. In addition, thermal or catalytic inefficiencies in the Sabatier reactor may result in even lower conversion and additional un-recovered O_2. However, relatively low reaction temperature (400°C) [4]and non-toxic and easy to handle byproducts make this technology amenable to space cabin environment.

Based on the stoichiometry, 50% of the hydrogen will be lost as methane unless utilized as a fuel or further treated in a carbon formation reactor to retrieve hydrogen. (Methane will be vented in the ISS air revitalization architecture). Hence, Sabatier-based process technology is less than ideal for long-term space exploration missions because of the loss of valuable resources such as hydrogen.[2]

Bosch technology offers complete recovery of oxygen with no hydrogen loss according to the reaction shown in Equation (2).

$$CO_2 + 2H_2 \rightarrow 2\,H_2O + C \quad (2)$$

In practice, however, carbon formation is a significant issue in a Bosch reactor. Multi-pass reactors are required to ensure complete conversions. Bosch reaction takes place over 600°C and frequent carbon removal and handling is required to avoid deposition of carbon on the catalyst. Assuming that the carbon handling is done in terms of catalyst cartridge replacement, increased consumable load could also be a potential issue with the Bosch reactor. The reactor needs to be cooled down and restarted for carbon removal. The technology is still at a low TRL level and further development is necessary to fit Bosch technology for long-duration life support applications. [5]

CO_2 electrolysis is a promising process, but offers only a partial oxygen recovery.

$$2CO_2 \rightarrow 2CO + O_2 \quad (3)$$

CO is a valuable product, if collected and stored to be utilized as fuel or propellant. Several methods of electrolysis have been studied, including solid-oxide electrolysis. It is a high temperature process (around 800°C) and materials compatibility and scale up issues have been holding back the progress of this technology. However, recent advances in the electrochemical and fuel cell industry have provided solutions to many technical challenges that impeded the development of electrochemical CO_2 reduction technologies.

The CO_2-H_2O co-electrolysis process developed by INL [6] is an advanced electrochemical process that involves simultaneous electrolysis of CO_2 and water vapor to produce CO and H_2 (syngas). The technology is a combined process that involves steam electrolysis, CO2 electrolysis, and the reverse water gas shift (RWGS) reaction. The process takes place at around 800°C.

The overall reaction is shown in Equation (4).

$$CO_2 + H_2O \rightarrow H_2 + CO + O_2 \quad (4)$$

The co-electrolysis technology combines the CO_2 reduction and oxygen generation processes into a single hardware efficiently to offer a significant mass reduction, in the air revitalization architecture. This technology has significant relevance for NASA to enable human space flight missions beyond low-earth orbit. In life support architecture, it will reduce the overall system mass by eliminating the need for a separate water electrolysis system. The co-electrolysis is an enabling technology in the *in situ* fuel production architecture, both for the human and robotic exploration of Mars. In general, employing common technologies for multiple applications improves the mission reliability and safety. This paper contains the preliminary results of a study to investigate the advantages of the co-electrolysis as a technology element that can be shared between life support and fuel production systems in future missions. Mathematical models of CO_2 and water co-electrolysis as an independent and auxiliary technology (in combination with the Sabatier and Bosch technologies) to compliment NASA's closed-loop air revitalization design are presented.

II. Background

The INL co-electrolysis process was developed primarily to produce synthetically driven hydrocarbon fuels from CO_2 as an alternative energy solution. Traditionally, synthetic fuels are produced from syngas, a mixture of hydrogen and carbon monoxide. The combined electrolysis of CO_2 and steam produce oxygen and syngas as shown in Equation (4). The INL co-electrolysis process is based on the solid-oxide electrolysis (SOE) technology. SOE is a high-temperature electrolysis process and is significantly more power-efficient compared to conventional low temperature electrolysis processes). The process takes place at around 800°C. The technology is a combined process that involves steam electrolysis, CO2 electrolysis, and the reverse water gas shift (RWGS) reaction.

As shown in Figure 2, Co-electrolysis has significant advantage over separate electrolysis of water and CO_2 in terms of electrical efficiency. Compared to pure CO_2 electrolysis, the co-electrolysis using a solid-oxide cell utilizes

considerably less electrical energy (only as much as the water electrolysis alone) since the carbon monoxide production in co-electrolysis occurs mainly due to RWGS.

A. Solid Oxide Electrolysis Cell

A solid oxide cell is a key component of the electrolysis system. It consists of an electrolyte and two electrodes as shown in Figure 3.[7] The electrolyte is a gas-tight ceramic membrane that can conduct ions and is sandwiched between two porous electrodes that can conduct electrons. In the solid-oxide fuel cell (SOFC), oxygen molecules dissociate at the oxygen electrode (cathode) and combine with electrons coming from external electric power source to form oxygen ions. The oxygen ions conduct through the electrolyte and migrate towards the hydrogen electrode (anode). The fuel (hydrogen or natural gas) is fed to the anode and reacts with the oxygen ions to form water and CO_2. The solid-oxide electrolysis cell operates in the reverse mode and the names and function of the electrodes are also reversed. The electrolysis and fuel cell modes of operation are represented in Figures 3 (a) and 3 (b), respectively.

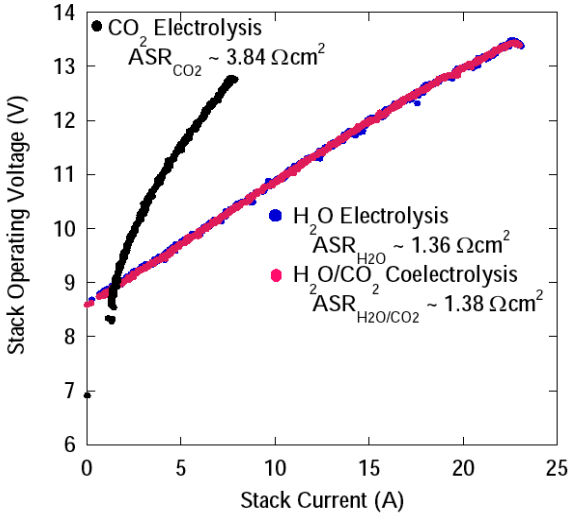

Figure 2. Electrical efficiency of co-electrolysis versus separate water and pure CO_2

The most common materials currently used for the solid oxide cells are listed in Table 1.[8] The electrolyte is a dense gas-tight ceramic layer, usually made from yttria stabilized zirconia (YSZ) with yttria content of 8 mol% to fully stabilize the electrolyte composition. The performance of the electrolyte depends on how well it can conduct oxide ions ($O^{=}$). The cell's ion conductivity decreases and hence the ohmic resistance increases with the thickness of the electrolyte.

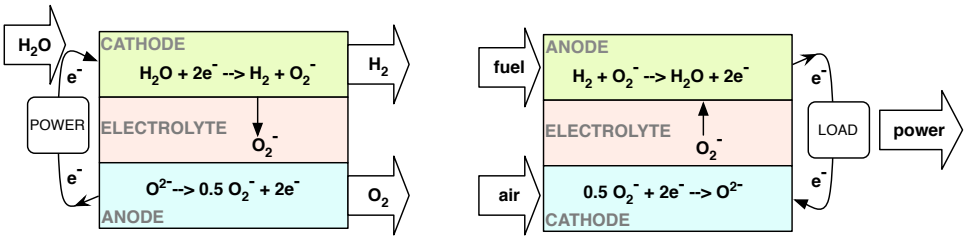

Figure 3. (a) Solid oxide electrolysis cell (SOEC) for water electrolysis; (b) solid oxide fuel cell (SOFC) operating in reverse compared to an SOEC [Guan et al. 2006].

The most common anode material for SOFC is a porous cermet (**cer**amic-**met**al), made from Ni and YSZ. Electronically conductive and gas-tight interconnect plates connect the individual cells to form a stack. The ionic conductivity of ceramics is highly dependent on the ceramic temperature. Thus, high

Table 1. Commonly used materials in SOFC/SOEC

component	material	acronym
Steam/hydrogen electrode	Ni - $Y_x\ Zr_{1-x}\ O_{2-x/2}$ (nickel-yttria stabilized zirconia)	Ni-YSZ
Electrolyte	$Y_x\ Zr_{1-x}\ O_{2-x/2}$ (yttria stabilized zirconia)	YSZ
Air/oxygen electrode	$Sr_xLa_{1-x}\ MnO_{3-\delta}$ + $Y_x\ Zr_{1-x}\ O_{2-x/2}$ (doped lanthanum manganite)	LSM-YSZ
Interconnect	Chromium based alloys/ceramics or stainless steel	SS

operating temperatures are required to obtain sufficient overall conductivity in the solid oxide cell. YSZ exhibits acceptable conductivity in the 700–1100ºC temperature range.

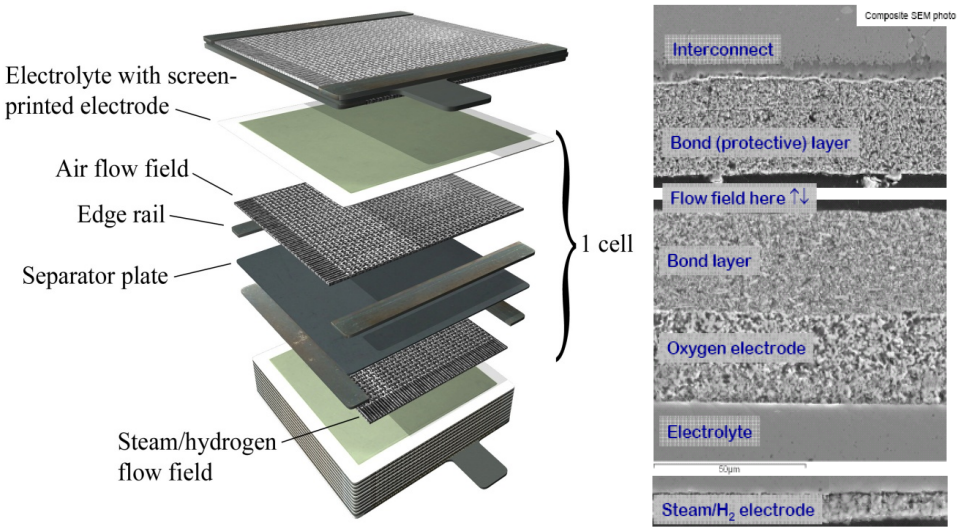

Figure 4. Ceramatec solid oxide cell/stack construction; (scanning electron microscopy, Reference 1)

In the fuel cell mode, air is fed to the cathode and the hydrogen is fed to the anode. At the cathode, where electrons are supplied via external electrical power, oxygen molecules are reduced to oxygen ions. The oxygen ions are conducted through the electrolyte to the anode. At the anode, oxygen ions oxidize the gaseous fuel to form water and carbon dioxide, while producing electricity as a result of the transport of free electrons back to the cathode through the external circuit. So, the properties of the anode and cathode are to be chosen such that they facilitate reduction of oxygen and oxidation of gaseous fuel. The solid oxide electrolyte acts as the barrier between the electrodes to separates the reduction and oxidation reactions. In the electrolysis mode, electrical energy is supplied so that the fuel cell process is reversed causing to electrolyze the steam to oxygen and hydrogen.

III. Process Model Development

The approach to this study was to develop and compare theoretical models of the CO_2 and steam co-electrolysis and other key CO_2 reduction processes such as Sabatier and Bosch to compare their performance in terms of oxygen production and CO_2 utilization. Integrated models of these key CO_2 reduction and co-electrolysis processes were also developed to investigate options to improve the efficiency of the resource recovery process. Sabatier technology was chosen primarily because it is the baseline CO_2 reduction technology for ISS. Even though the carbon handling issue is still a concern, Bosch technology remains attractive due to its potential to maximize oxygen recovery.

Traditional operation of a Bosch system operates at 650°C to form water and solid carbon through the reduction of carbon dioxide with hydrogen in a single reactor. The formation of water and carbon occurs through three reactions, including the Reverse Water-Gas Shift reaction, the Boudouard reaction, and carbon monoxide Hydrogenation, as shown in Equations (5) through (7).

$$CO_2 + H_2 \rightarrow H_2O + CO \text{ (RWGS)} \quad (5)$$

$$2CO \rightarrow CO_2 + C \text{ (Boudouard)} \quad (6)$$

$$CO + H_2 \rightarrow H_2O + C \text{ (Hydrogenation)} \quad (7)$$

Bosch reactors, however, has practical issues related to catalyst fouling, high operating temperature, and large volume and mass requirements due to low single-pass conversions. Separation of the traditional single-reactor Bosch system into a series-reactor system may significantly reduce the temperature, volume, and mass requirements. Additionally, catalyst fouling may be minimized through distribution in a series-reactor system. For a series-reactor system, the first reactor would be used exclusively to produce carbon monoxide through the RWGS reaction. The second reactor would be devoted to carbon formation either through the Boudouard reaction, CO Hydrogenation, or

a combination of the two. Due to the significant cost associated with designing and building reactors, modeling of such a system was of key interest and hence the Boudouard and hydrogenations models were also investigated under this study. Individual process models for Sabatier, Bosch, Boudouard, and hydrogenation reactions used the room-temperature electrolysis, which is the solid polymer electrolysis (SPE) technology, as the basis to generate hydrogen and oxygen from water.

The process models for this study were developed using Hyprotech's HYSYS.Plant v2.2.2 (Build 3806) process modeling software. HYSYS.Plant ensures mass and energy balances across all components inherently and includes thermodynamic data for all chemical species. The software models components such as pumps, compressors, turbines, and heat exchangers realistically. It also models chemical equilibrium and kinetic reactions. The models described in this paper were developed assuming steady state operation with chemical equilibrium reactions.

IV. Results

The process flow diagram for the Bosch process is shown in Figure 5. In this model, the Bosch system receives CO_2 at 172kPa (25psia) from the LPCOR system. The CO_2 is then mixed with hydrogen and a recycle stream that consists of hydrogen, carbon monoxide, methane and some water vapor. The mixed stream is heated using a recuperating heat exchanger to the reaction temperature of 650°C before it enters the Bosch reactor. The Bosch reactor is simulated using two reactors, the Gibbs and Chemical Equilibrium reactors as shown in Figure 6. In the Gibbs reactor, the Gibbs free energy of selected products and reactants are minimized to estimate the most likely equilibrium composition. The reactants and the products of the Gibbs reactor include water, methane, carbon monoxide, carbon dioxide and hydrogen. The Gibbs reaction is primarily the reverse water gas shift reaction with some methanation, shown in Equations (8) and (9).

$$CO_2 + H_2 \leftrightarrow CO + H_2O \tag{8}$$

$$CO + 3H_2 \leftrightarrow CH_4 + H_2O \tag{9}$$

The Chemical Equilibrium reactor in the Bosch system model simulates the Boudouard reaction as shown in Equation (10).

$$2CO_2 \leftrightarrow CO_2 + C \tag{10}$$

This model used a tabular chemical equilibrium data. The Gibbs reaction is endothermic and the Boudouard reaction is exothermic, which makes the overall Bosch reaction exothermic.

The Bosch reactor produces solid carbon and a gas stream. The percent conversion of carbon per pass is determined based on the molar flow of carbon monoxide into the Bosch reactor and the carbon flow out of the reactor. The model assumed 10% conversion and in order to maintain this requirement, the approach temperature to the Boudouard reactor was adjusted artificially to limit the conversion per pass. The hot gas stream exiting the reactor passes through a recuperating heat exchanger and gets cooled while preheating the stream that enters the reactor. The traces of water vapor in the gas stream further cooled in a condenser using ambient cooling. The condensed water is mixed with the main water stream and electrolyzed to product hydrogen and oxygen. The cooled gas stream exiting the water condenser is recycled with the incoming carbon dioxide and hydrogen streams. This recycled stream contains hydrogen, methane, carbon monoxide, carbon dioxide and some water. The hydrogen to carbon dioxide ratio was set to 2:1 by adjusting the incoming water stream. In this model, the composition of the recycle stream was adjusted so that the ratio of recycle flow to the combined hydrogen and carbon dioxide flow close to 14.

The electrolysis process is modeled, as shown in Figure 7, assuming 100% conversion based on Equation (11).

$$2H_2O \rightarrow 2H_2 + O_2 \tag{11}$$

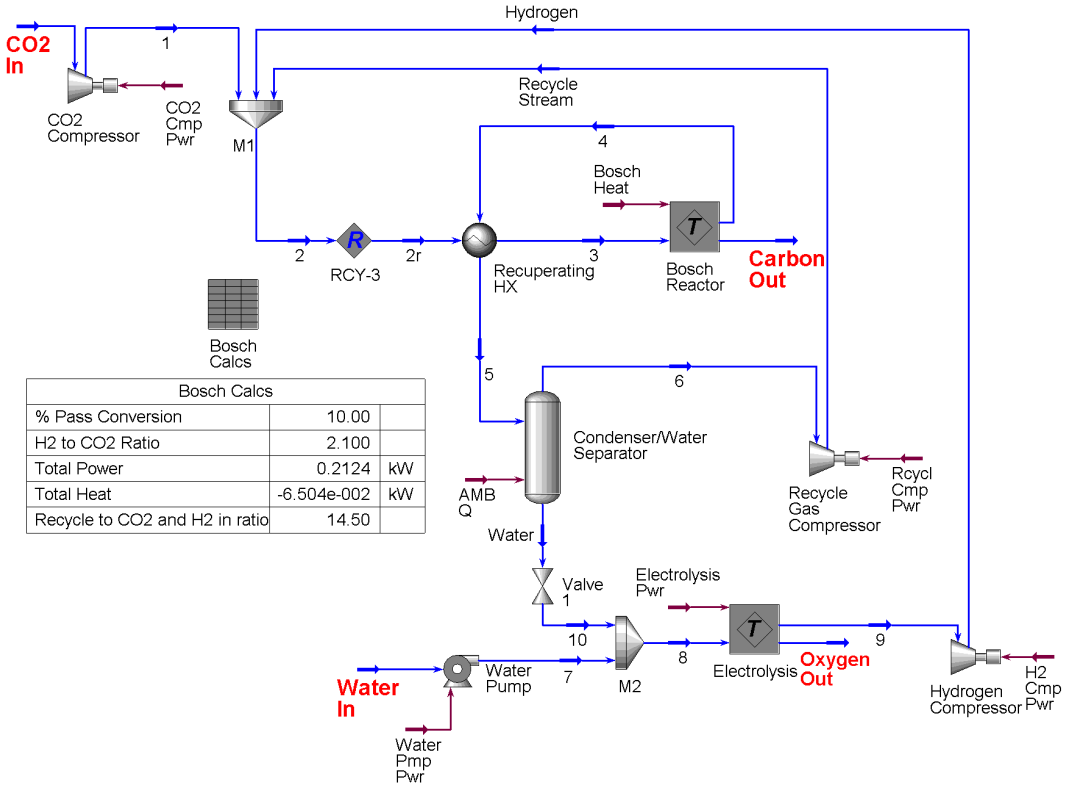

Bosch Calcs		
% Pass Conversion	10.00	
H2 to CO2 Ratio	2.100	
Total Power	0.2124	kW
Total Heat	-6.504e-002	kW
Recycle to CO2 and H2 in ratio	14.50	

Figure 5. Process flow diagram of Bosch process

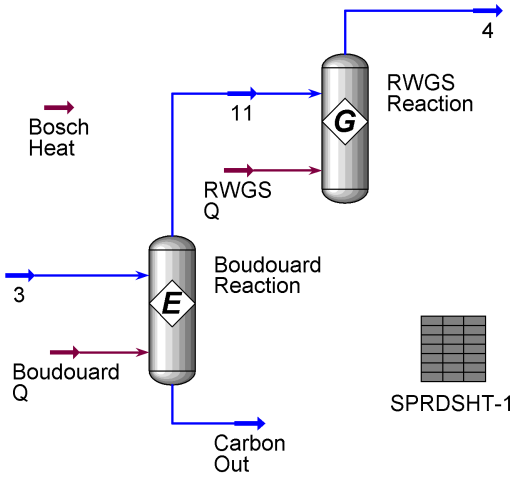

Figure 6.

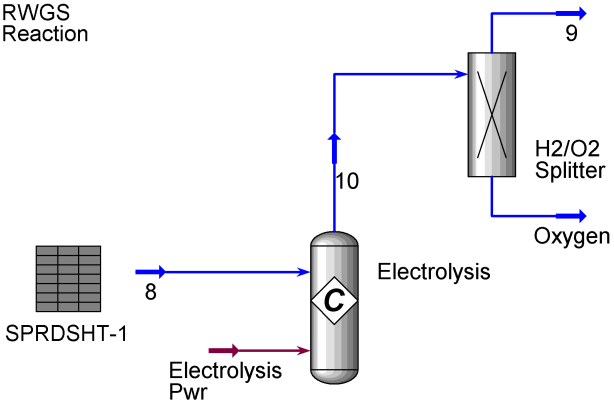

Figure 7.

Flow diagrams of Bosch (Figure 6) and co-electrolysis (Figure 7) processes

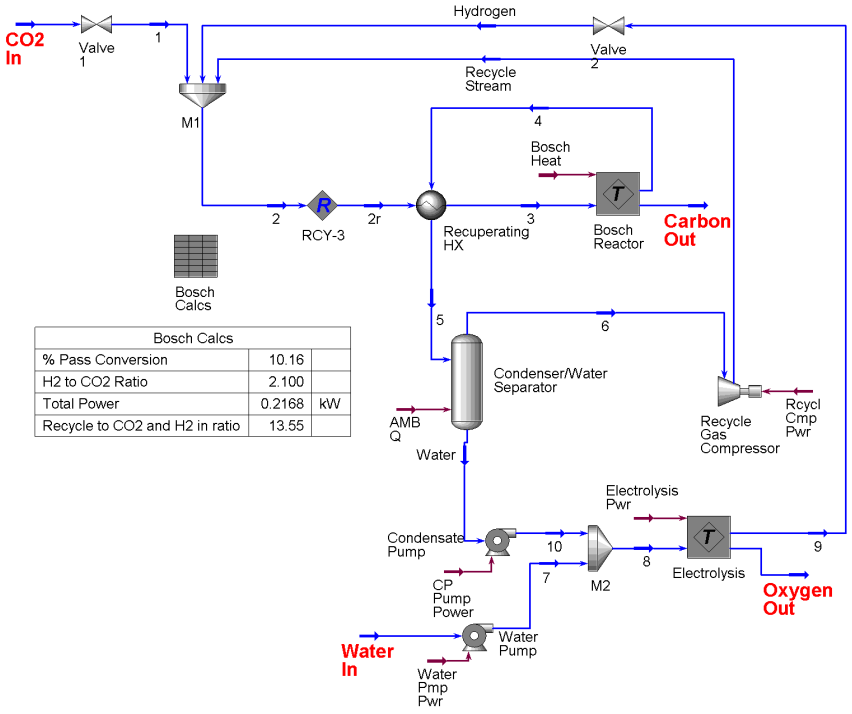

Figure 8. Process flow diagram of Bosch process at sub-atmospheric conditions

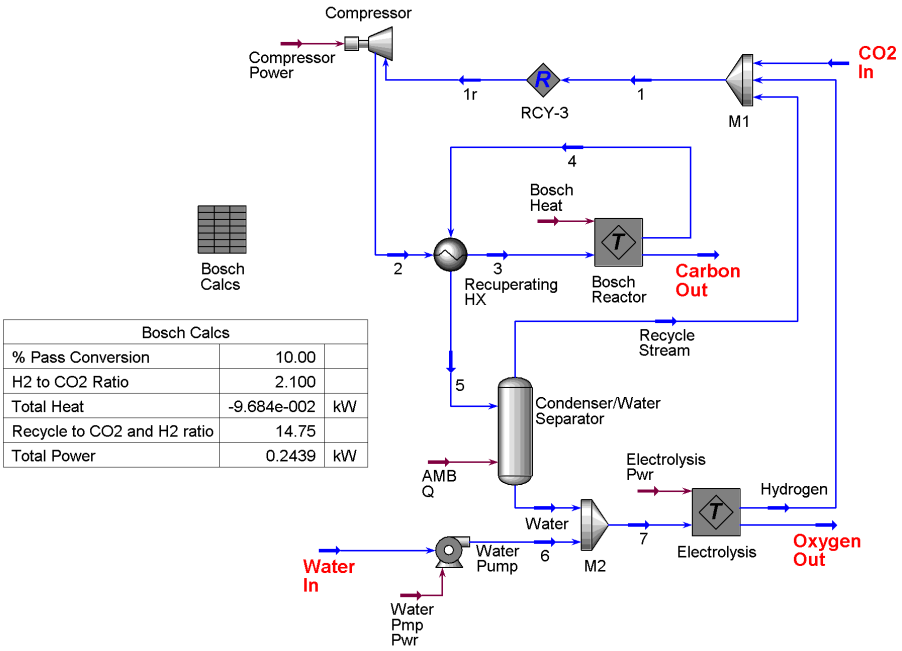

Figure 9. Process flow diagram of Bosch process with single compressor

The HYSYS calculates the power necessary to split the water. A component splitter follows to separate the oxygen from the hydrogen. The electrolysis process conditions are set to near ambient conditions. Figure 8 represents a slightly modified Bosch process flow model. The Bosch reactor in this case operates at sub-atmospheric conditions and the electrolysis process operates at atmospheric conditions. Pumps are used instead of compressors for this model. The final modification to the basic Bosch process model is the replacement of the three compressors with one compressor, as shown in Figure 9. This model represents a Bosch system with minimum number of process equipment, in terms of the number of compressor.

B. Sabatier Process Model

The Sabatier process is shown in Figure 10. In this model, the Sabatier reactor receives a combined stream of CO_2 and hydrogen from LPCOR and the electrolysis unit, respectively at 79kPa (11.5psia). The process flow diagram of the model is shown in Figure 10.

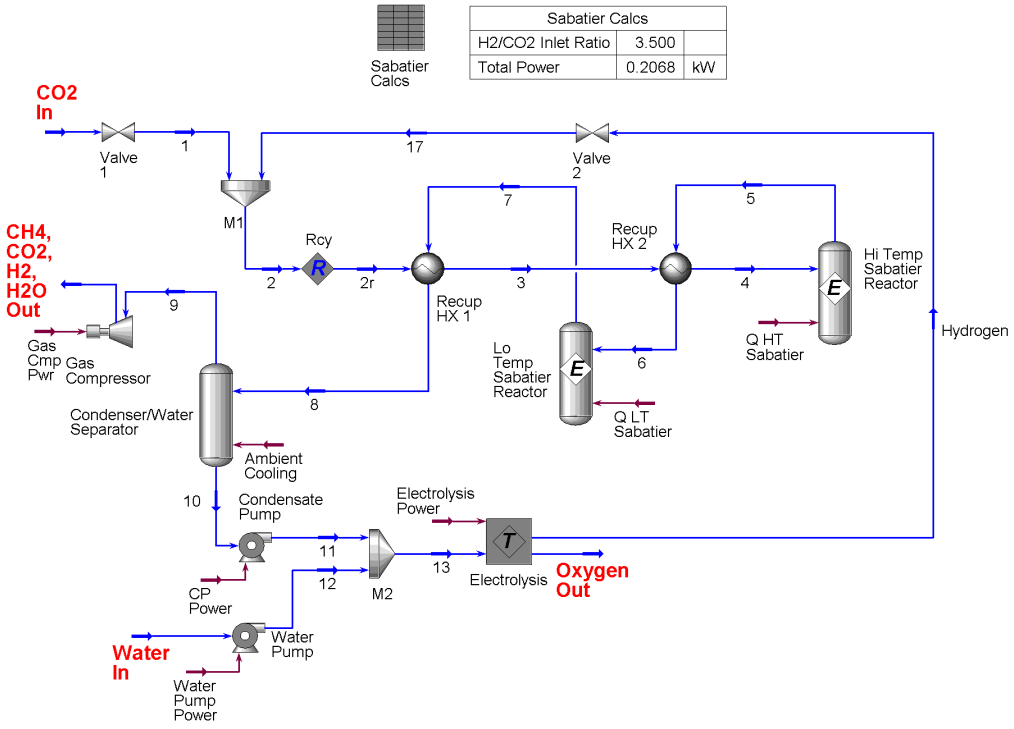

Figure 10. Process flow diagram of base Sabatier process

The overall Sabatier reaction is simulated by using two equilibrium reactors, a lower temperature reactor at 240°C and a higher temperature reactor at 565°C. Heat recuperation occurs at the inlet and outlet of the total reactor and in between the two equilibrium reactors. The equilibrium reactors calculate the outlet compositions based on a default tabulated methanation data within the HYSYS.Plant software. The outlet stream from the Sabatier reactor is cooled and is water condensed within the water knockout tank (condenser). The condensate is added to main water stream before entering the water electrolyzer. The gas stream exiting the water knockout tank is compressed to atmospheric conditions and released. This gas stream primarily contains methane and some carbon dioxide and water and trace amounts of hydrogen. The Sabatier and Bosch models use the same electrolysis process model. The hydrogen to carbon dioxide ratio for this model was maintained at 3.5 by adjusting the water inlet flow.

C. Co-Electrolysis Integrated Process Models

1. 1-D Co-Electrolysis Model

A one-dimensional chemical equilibrium model was developed for the analysis of steam and CO_2 co-electrolysis. This model can be used to predict open-cell and operating potentials, electrolyzer outlet compositions, and outlet temperatures for specified inlet gas flow rates, current densities, cell area-specific resistance, and thermal boundary condition.

The Nernst potential for the co-electrolysis system can be calculated as a function of temperature using the Nernst equation for either steam-hydrogen or for CO_2-CO systems, provided the equilibrium composition of the components is used in evaluating the equation. Therefore, prior to applying the Nernst equation, the electrolyzer inlet equilibrium composition must be determined at the operating temperature. The chemical equilibrium co-electrolysis model determines the equilibrium composition of the system as follows.

The overall water gas shift reaction that occurs during heating from the cold unmixed inlet state to the hot mixed pre-electrolyzer state can be represented as shown in Equation (12).

$$y_{0,CO}\,CO + y_{0,CO2}\,CO_2 + y_{0,H2}\,H_2 + y_{0,H2O}\,H_2O \rightarrow y_{1,CO}\,CO + y_{1,CO2}\,CO_2 + y_{1,H2}\,H_2 + y_{1,H2O}\,H_2O \qquad (12)$$

The $y_{0,j}$ values represent the cold inlet mole fractions of CO, CO_2, H_2, and H_2O, respectively, that are known from specification of the individual component inlet gas flow rates. The unknown equilibrium mole fractions of the four species at the electrolyzer temperature prior to electrolysis are represented by the $y_{1,j}$ values. There are three governing chemical balance equations for carbon, hydrogen, and oxygen corresponding to Equation (12), as shown in Equations (13, 14, and 15).

$$y_{0,CO} + y_{0,CO2} = y_{1,CO} + y_{1,CO2} \qquad (13)$$

$$2y_{0,H2} + 2y_{0,H2O} = 2y_{1,H2} + 2y_{1,H2O} \qquad (14)$$

$$y_{0,CO} + 2y_{0,CO2} + y_{0,H2O} = y_{1,CO} + 2y_{1,CO2} + y_{1,H2O} \qquad (15)$$

The final Equation invokes the equilibrium constant for the shift reaction is represented by (16).

$$K_{eq}(T) = \frac{y_{1,CO2}\,y_{1,H2}}{y_{1,CO}\,y_{1,H2O}} \qquad (16)$$

Simultaneous solution of Equations (13) through (15) yields the hot inlet composition.
Once the hot inlet equilibrium composition is determined, the open-cell Nernst potential can be calculated from Equation (17).

$$V_N = \frac{-\Delta G_{f,H_2O}(T)}{2F} - \frac{R_u T}{2F}\ln\left[\left(\frac{y_{1,H2O}}{y_{1,H2}\,y_{O2}^{1/2}}\right)\left(\frac{P}{P_{std}}\right)^{-1/2}\right] = \frac{-\Delta G_{f,CO_2}(T)}{2F} - \frac{R_u T}{2F}\ln\left[\left(\frac{y_{1,CO2}}{y_{1,CO}\,y_{O2}^{1/2}}\right)\left(\frac{P}{P_{std}}\right)^{-1/2}\right] \qquad (17)$$

y_{O2} represents the mole fraction of oxygen on the air-sweep side of the cells ($y_{O2} \sim 0.21$). Note that the Nernst equation for either steam-hydrogen or CO_2-CO yields the same result for the equilibrium system.

The electrolyzer outlet composition can be determined similarly, after accounting for electrochemical reduction of the system. The chemical balance equation for oxygen must be modified to account for oxygen removal from the CO_2 and steam mixture. Accordingly, the oxygen balance can be represented as in Equation (18).

$$y_{1,CO} + 2y_{1,CO2} + y_{1,H2O} = y_{2,CO} + 2y_{2,CO2} + y_{2,H2O} + \Delta n_O \qquad (18)$$

Δn_O is the relative molar rate of monatomic oxygen removal from the CO_2/steam mixture given by Equation (19).

$$\Delta n_O = \frac{I_e}{2F\dot{N}_{Tot}} \tag{19}$$

In this Equation, I_e is the total ionic current, $I_e = i \cdot A_{cell} \cdot N_{cells}$, $\dot{N}_{Tot}$ is the total molar flow rate on the CO_2 and steam side, including any inert gas flows, and F is the Faraday number. Finally, using the modified oxygen balance equation, the post-electrolyzer equilibrium composition (state 2) can be determined as a function of temperature from simultaneous solution of three chemical balance equations and the equilibrium constant equation.

In general, the electrolyzer outlet temperature is unknown. The magnitude of any temperature change associated with electrolyzer operation depends both on the operating conditions (operating voltage, inlet composition, gas flow rates, etc.) and on the thermal boundary condition. If the electrolyzer operating voltage is below the thermal neutral voltage, the endothermic reaction heat requirement dominates and the stack will tend to cool off. If the operating voltage is above thermal neutral, ohmic heating dominates and the stack tends to heat up.

If adiabatic electrolyzer operation is assumed, the outlet temperature can be determined as a function of operating voltage from simultaneous solution of the energy equation and the chemical balance and equilibrium constant equations. Alternately, if isothermal operation is assumed, the outlet composition can be determined independently of the energy equation and the heat required to maintain isothermal operation can be calculated as a function of operating voltage.

For pure-steam or pure-CO_2 electrolysis, the thermal neutral voltage is given by Equation (20).

$$V_{tn,j}(T) = \frac{\Delta H_{R,j}(T)}{2F} \tag{20}$$

$\Delta H_{R,j}(T)$ is the enthalpy of reaction for electrolysis of pure component j (H_2O or CO_2) at temperature T. At 800°C, $V_{tn,H2O}$ = 1.29 V and $V_{tn,CO2}$ = 1.46 V. For co-electrolysis, the thermal neutral voltage can range anywhere between the respective pure-component values, depending on inlet composition, oxygen utilization, and temperature (via the equilibrium constant, $K_{eq}(T)$). There is no simple explicit relation for the multi-component thermal neutral voltage. In general, the thermal neutral voltage for coelectrolysis will be closer to the pure-steam value if the inlet composition is dominated by steam and hydrogen. Conversely, if the inlet composition is dominated by CO_2 and CO, the coelectrolysis thermal neutral voltage will be closer to the pure-CO_2 value. At an operating temperature of 800°C, with syngas-production-relevant inlet compositions for coelectrolysis (i.e., ~2-to-1 steam/hydrogen vs CO_2), a thermal neutral voltage value of ~1.34 V is typical.

The energy equation for the coelectrolysis process is represented by Equation (21).

$$\dot{Q} - \dot{W} = \sum_P \dot{N}_i [\Delta H^o_{f_i} + H_i(T_P) - H^o_i] - \sum_R \dot{N}_i [\Delta H^o_{f_i} + H_i(T_R) - H^o_i] \tag{21}$$

$\dot{Q}$ is the external heat transfer rate to or from the electrolyzer, $\dot{W}$ is the rate of electrical work supplied to the electrolyzer, $\dot{N}_i$ is the molar flow rate of each reactant or product, $\Delta H^o_{f_i}$ is the standard-state enthalpy of formation of each reactant or product and $H_i(T) - H^o_i$ is the sensible enthalpy for each reactant or product. Applying the energy equation in this form, all reacting and non-reacting species in the inlet and outlet streams are accounted for, including inert gases, process steam, hydrogen (introduced to maintain reducing conditions on the steam/hydrogen electrode), CO_2, and any excess un-reacted process gases.

In general, determination of the outlet temperature from Equation (21) is an iterative process. The heat transferred during the process must first be specified (e.g., zero for the adiabatic case). The temperature-dependent enthalpy values of all species must be available from curve fits or some other database. The cathode-side hot electrolyzer-inlet molar composition and flow rates of steam, hydrogen, CO_2, CO, and any inert carrier gases such as

nitrogen (if applicable) have already been determined from specification of the cold inlet flow rates of all components and from Equations (13 – 17). The inlet flow rate of the sweep gas (e.g., air or steam) on the anode side must also be specified. At this point, the total electrolyzer-inlet enthalpy given by the second summation on the right-hand side of Eqn. (14) can be evaluated. The current density, active cell area, and number of cells are then specified, yielding the total ionic current, I_e. Care must be taken to insure that the specified inlet gas flow rates and total ionic current are compatible. The minimum required inlet steam and CO_2 molar flow rates must satisfy the constraint represented by Equation (22) to avoid starvation.

$$\dot{N}_{H_2O} + \dot{N}_{CO_2} \geq \frac{I_e}{2F} \tag{22}$$

The oxygen contribution from the CO_2 is only counted once, since we want to avoid creation of carbon soot, which could foul the cells.

Evaluation of the electrolyzer-outlet total enthalpy, the first summation in Eqn. (14), requires the product temperature, but the product temperature is generally unknown and is determined from solution of the energy equation, so an iterative solution must be applied. The iterative solution process proceeds as follows. Based on a guessed value of electrolyzer outlet temperature, T_P, and the specified current, the electrolyzer outlet composition can be determined as described previously, allowing for evaluation of the total enthalpy of the products.

The remaining term in the energy equation is the electrical work, which is the product of the per-cell operating voltage and the total ionic current. The operating voltage corresponding to the specified current density is obtained from Equation (23).

$$V_{op} = \overline{V}_N + i \times ASR(T) \tag{23}$$

The stack area-specific resistance, *ASR(T)*, quantifies the loss mechanisms in the operating cell. It must be estimated, based on experimental data or an appropriate model, and specified as a function of temperature. The operating-cell mean Nernst potential, $\overline{V}_N$, accounting for the variation of gas composition and temperature across the operating cell, can be obtained from an integrated form of the steam-hydrogen-based (or the CO_2-CO-based) Nernst equation, as per Equation (24).

$$\overline{V}_N(T_P) = \frac{1}{2F(T_P - T_R)(y_{2,O_2} - y_{1,O_2})[y_{2,H_2}(T_P) - y_{1,H_2}]} \times \int_{T_R}^{T_P} \int_{y_{1,O2}}^{y_{2,O2}} \int_{y_{1,H2}}^{y_{2,H2}(T_P)} \Delta G_{R,H_2O}(T) + R_u T \ln\left(\frac{1 - y_{H_2} - y_{0,CO_2} - y_{N_2}}{y_{H_2} y_{O_2}^{1/2}}\right) dy_{H_2} dy_{O_2} dT \tag{24}$$

The variable in this Equation is the unknown product temperature, T_P, which appears both explicitly and implicitly in the upper integration limits. The steam mole fraction has been expressed in the integrand numerator in terms of the hydrogen mole fraction. The mole-fraction subscripts 0, 1, 2 again refer to the cold inlet, hot electrolyzer inlet, and the hot electrolyzer outlet states, respectively. Mole fractions at states 0 and 1 are fully defined. The state-2 mole fractions are based on the specified current density and the guessed value for T_P.

Once the mean Nernst potential is evaluated based on a guessed value for T_P, the operating voltage can be determined and the energy equation can be evaluated. The final converged solution for T_P must simultaneously satisfy the chemical balance Equations (13, 14, and 18), the equilibrium constant Equation (13), and the energy Equation (21), subject to Equations (23 through 24).

The solution methodology described above can be applied to any specified electrolyzer heat loss or gain. For adiabatic operation, $Q = 0$. Alternately, if the heat loss or gain from the operating electrolyzer is known from a separate heat transfer analysis for a given operating point, the value of that heat loss or gain would be used.

For isothermal electrolyzer operation, once the inlet flow rates, current density, and operating temperature are specified, an iterative solution is not necessary and the triple integral of Equation (17) reduces to a double integral

with known upper limits of integration. The energy Equation (21) can be solved directly for the heat required to maintain isothermal operation at any operating point.

The CEC model allows for accurate determination of coelectrolysis outlet temperature, composition (anode and cathode sides), mean Nernst potential, operating voltage and electrolyzer power based on specified inlet gas flow rates, heat loss or gain, current density, and cell *ASR(T)*. Alternately, for isothermal operation, it allows for determination of outlet composition, mean Nernst potential, operating voltage, electrolyzer power, and the isothermal heat requirement for specified inlet gas flow rates, operating temperature, current density and *ASR(T)*.

2. Implementation of co-electrolysis model into HYSYS

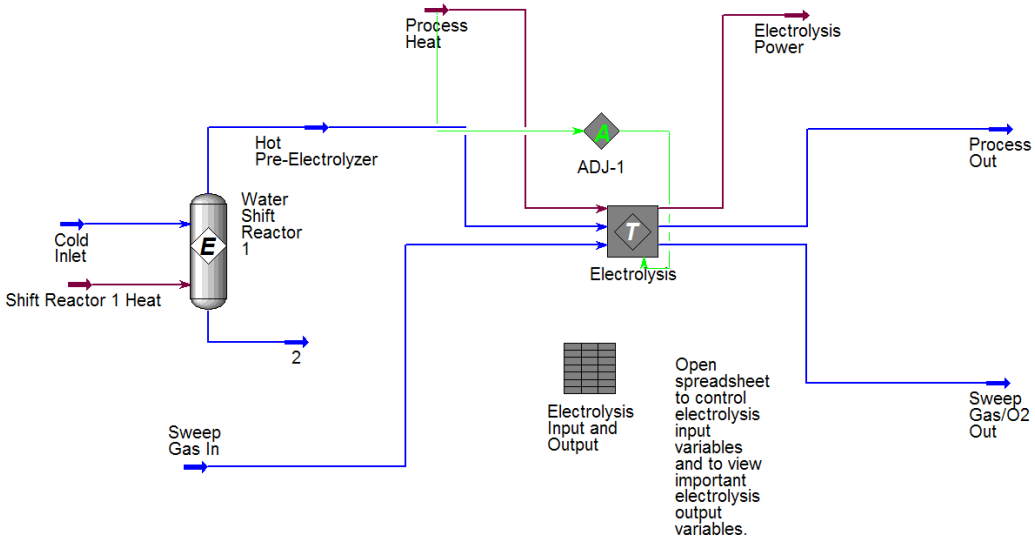

Figure 11. Process flow diagram external to the electrolysis module

Implementation of the co-electrolysis (CEC) model in HYSYS was done by taking advantage of as many built-in features of the systems-analysis code as possible. Figure 11 provides a process flow diagram (PFD) representing the implementation of the CEC model in HYSYS. The user-specified cold inlet process-gas stream enters at the left. This stream is equilibrated at the desired electrolyzer inlet temperature by means of an equilibrium reactor module that supports the shift reaction as per Equation (12). The hot streams of the shifted and sweep gases enter the electrolysis module. This electrolysis module was developed elsewhere for pure steam electrolysis application.

At this level of the model, the user may specify whether the electrolysis process will be isothermal or adiabatic. If the process is isothermal, the temperature of the process outlet stream must be specified, otherwise, the outlet temperature is determined by iteration using an embedded adjust logical (shown as the A within the diamond in Figure 11) until the process heat is zero. Also at this level, an embedded spreadsheet is used to input the electrolysis variables (current density, number of cells, cell area, area specific resistance, etc.).

The process flow diagram for the electrolysis module is shown in Figure 12. The, shifted, hot process stream enters a conversion reactor where the steam and/or carbon dioxide are electrolytically reduced. The conversion reactor unit includes both the steam and carbon dioxide reduction reactions.

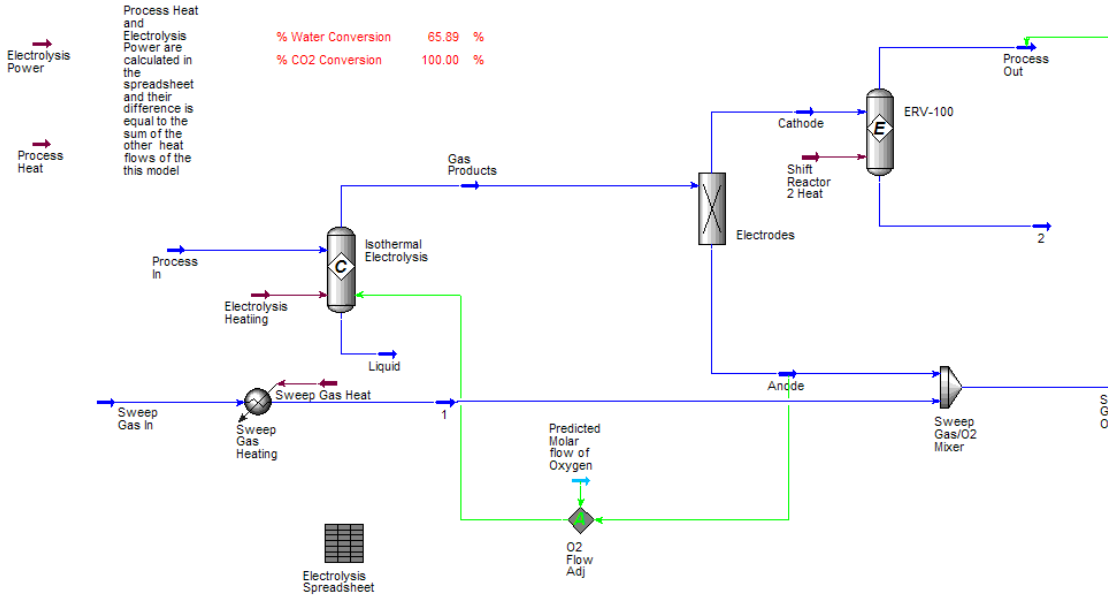

Figure 12. Process flow diagram for the electrolysis module with HYSYS

Based on the percent conversion of the steam and CO_2, the reactor will calculate the heat of reaction. The percent conversion of steam and (or) CO_2 is determined by the amount of oxygen generated using Equation (16). This value of the molar flow rate of oxygen produced is stored in a dummy stream. A logical adjust is used to change the percent conversion of steam and carbon dioxide until the oxygen molar flow rate leaving the conversion reactor is the same as the calculated value. The oxygen is split from the rest of the reacted process-gas components by means of a component splitter unit (labeled as "Electrodes" in Figure 12). The split oxygen combines with the sweep gas. The remaining components are passed through a second shift reactor to determine the outlet equilibrium composition.

As mentioned earlier, the outlet temperature of both the process and sweep streams are specified, but allowed to adjust if adiabatic conditions are desired. An embedded spreadsheet is used to evaluate the mean Nernst potential, as per Equation (24). Assuming a functional relationship for the Gibbs energy of formation, the definite integral was simplified analytically and this simplified version was programmed into the spreadsheet. Having defined the electrolysis variables, the amount of oxygen production is calculated in the spreadsheet using Equation (19). Based on an assumed outlet temperature, HYSYS proceeds to calculate all the thermodynamics and chemical reactions of the process resulting in outlet compositions for the process and sweep streams. Then the spreadsheet can calculate the mean Nernst potential by evaluating the simplified triple integral as per Equation (24). The operating voltage is obtained from Equation (23) and the electrolysis power is calculated by multiplying the operating voltage with the total current. HYSYS inherently assures that the energy balance as per Equation (21) is satisfied, which allows the process heat to be calculated by summing the electrolysis power with the total enthalpy differences from the electrolysis process and from the second shift reactor. If the outlet temperature is specified to be the same as the inlet temperature (isothermal operation), the calculation is complete and the process heat is known. If the process is specified to be adiabatic, the outlet temperature is adjusted until the process heat is zero. The process flow sheet automatically assures mass and energy balances.

3. Co-electrolysis integrated Sabatier process: with heat recuperation option

The Sabatier-co-electrolysis integrated model was developed by replacing the default elctrolysis process with the co-electrolysis module. The overall process was also modified so that water is mixed with the incoming carbon dioxide before the co-electrolysis process, as shown in Figure 13. Recycled water is combined with the incoming, main water stream and preheated through the low temperature recuperating heat exchanger. Carbon dioxide is mixed

with the water and some hydrogen and carbon monoxide from the exit stream of co-electrolysis process. Hydrogen and carbon monoxide constitutes approximately 10% of the molar composition of the inlet stream into the electrolysis process. The purpose of this is to provide reducing conditions at the hydrogen side (anode) of the solid oxide electrolysis cells. The recuperated heat from the exothermic Sabatier reactor further heats the stream to a vapor, which passes through a gas circulator to the high temperature recuperating heat exchanger. Although the heat transfer from the Sabatier reactors is not shown directly on the process flow diagram, an embedded spreadsheet was used to sum up the heats of both Sabatier reactors and the resulted amount of heat is used to operate the Sabatier heater. The gas is heated to over 700°C. However, it needs further heating through a high temperature electric heater to reach the electrolysis temperature of 800°C.

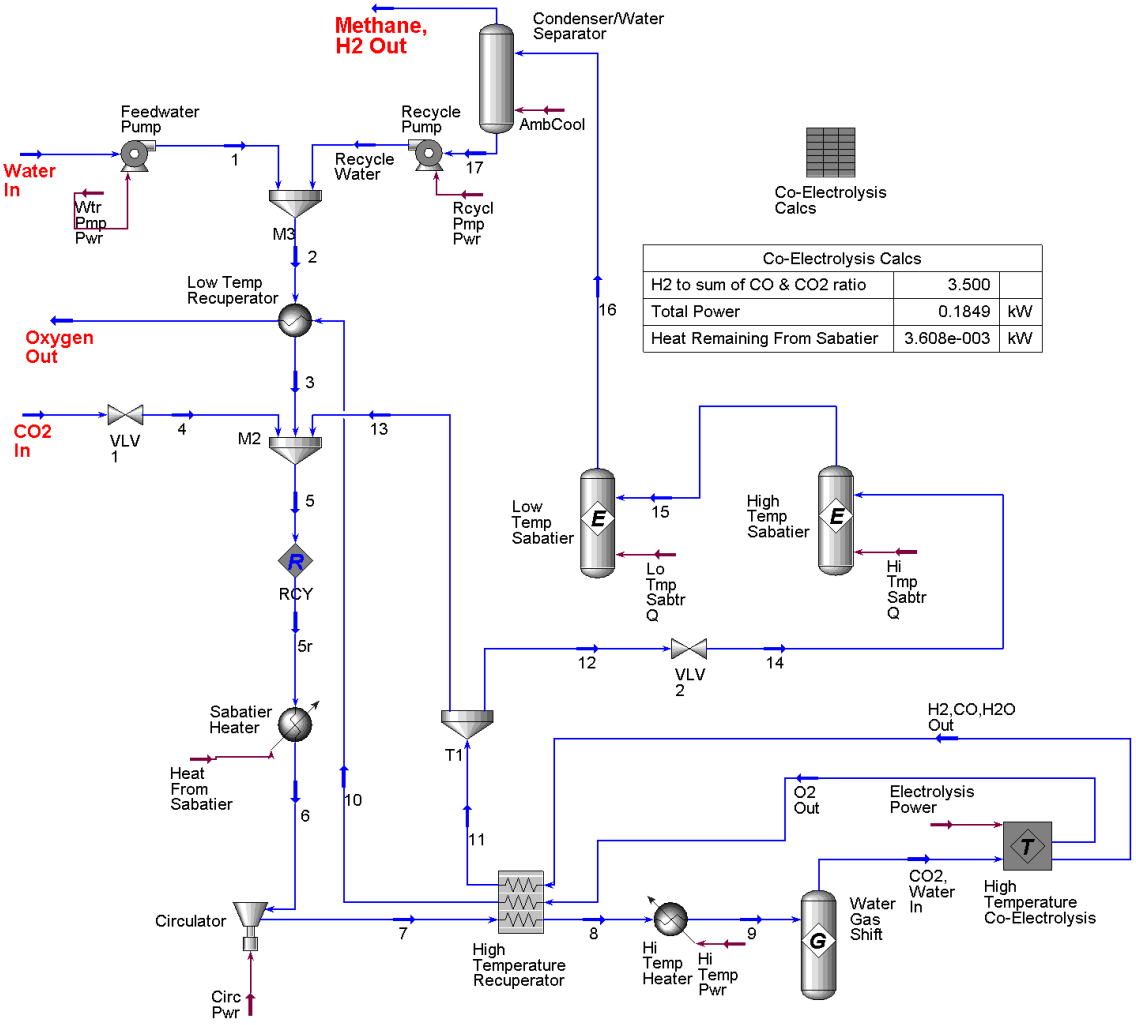

Figure 13. Process flow diagram of co-electrolysis integrated Sabatier process

The gases as they enter the electrolysis unit shift composition at this temperature. The metals that make up the solid oxide electrolyzer cells act as a catalyst for this water gas shift reaction. This is simulated in the model by using a Gibb reactor. The products leaving the co-electrolysis unit are primarily hydrogen and carbon monoxide with traces of water and carbon dioxide. The oxygen also exits the electrolysis module in another stream. Both

stream are at 800°C and are therefore used as the heat source for the high temperature recuperating heat exchanger. The oxygen stream is further cooled to near ambient conditions in the low temperature recuperative heat exchanger, which preheats the incoming water. A little over 10% of the hydrogen and carbon dioxide stream is mixed with the incoming water and carbon dioxide and the remaining 90% go through the Sabatier reactor where it is converted to methane and water. The water is condensed in the condenser/separator and mixed with fresh water (main water stream). The methane with some hydrogen and water vapor is discharged out at the vapor side of the condenser/separator. The ratio of hydrogen flow to the combined inlet carbon dioxide and carbon monoxide flow was set to 3.5 by adjusting the water inflow.

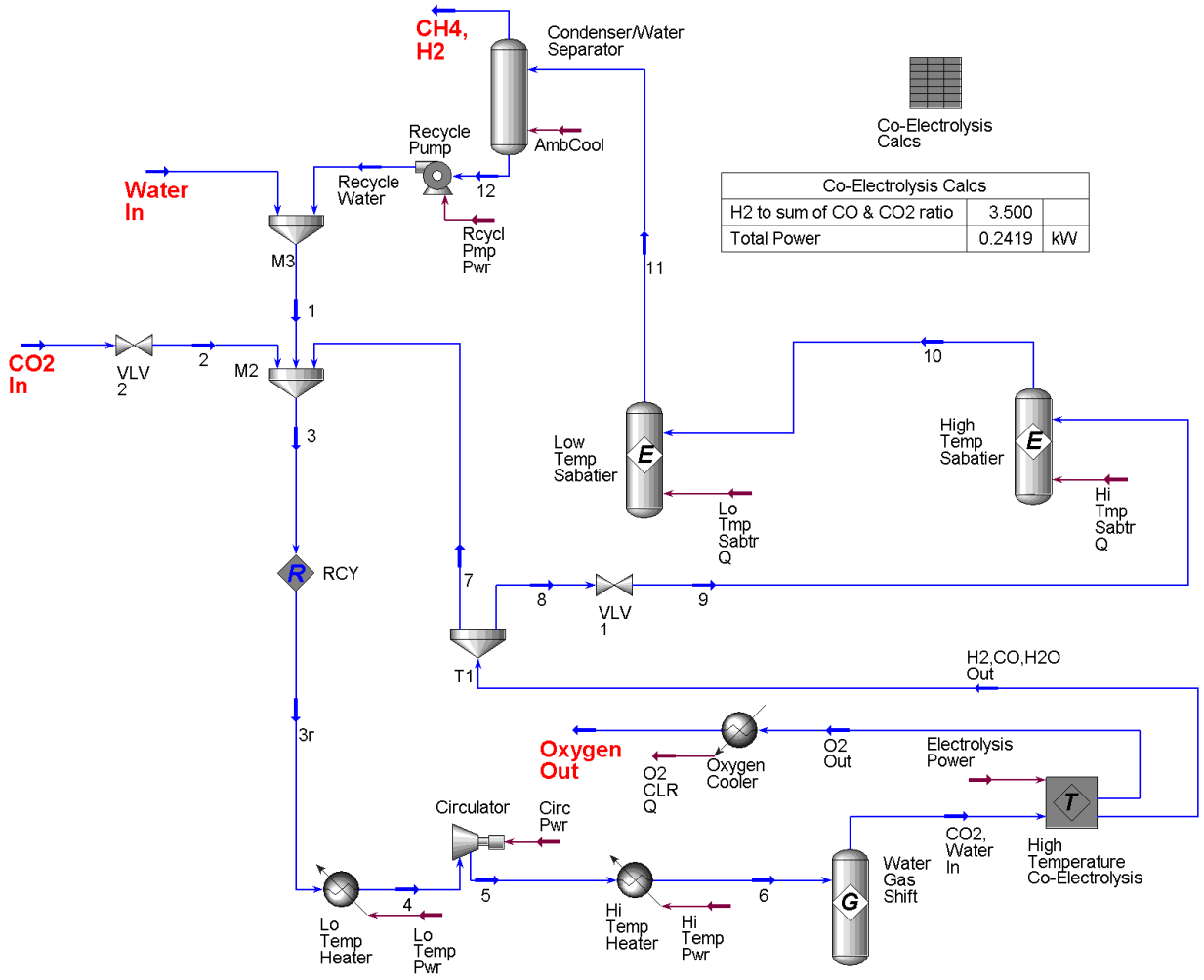

Figure 14. Process flow diagram of Sabatier process with co-electrolysis without heat recuperation

4. Co-electrolysis integrated Sabatier process: without heat recuperation option

The integrated model of Sabatier and co-electrolysis processes was modified in which no heat recuperation option is included. The model is shown in Figure 14. This was done to determine the maximum amount or power that would be needed to make the Sabatier and co-electrolysis integrated process work. Water, carbon dioxide, and

the syngas stream from the electrolysis unit are combined, compressed through the circulator, and electrically heated to the electrolysis temperatures before passing through the electrolyzer. The syngas passes through the Sabatier reactors to make methane and water. The water is condensed and mixed with incoming water and the methane, and some hydrogen is discarded. The oxygen exiting the electrolyzer is cooled by an ambient cooler.

5. Boudouard and Co-electrolysis integrated model

The Bosch process was modified by removing the water gas shift reactor and combined with the high-temperature co-electrolysis process as shown in Figure 15. Carbon dioxide is fed to the Boudouard reactior at 172kPa (25 psia) and is heated by the hot oxygen product from the electrolysis unit.

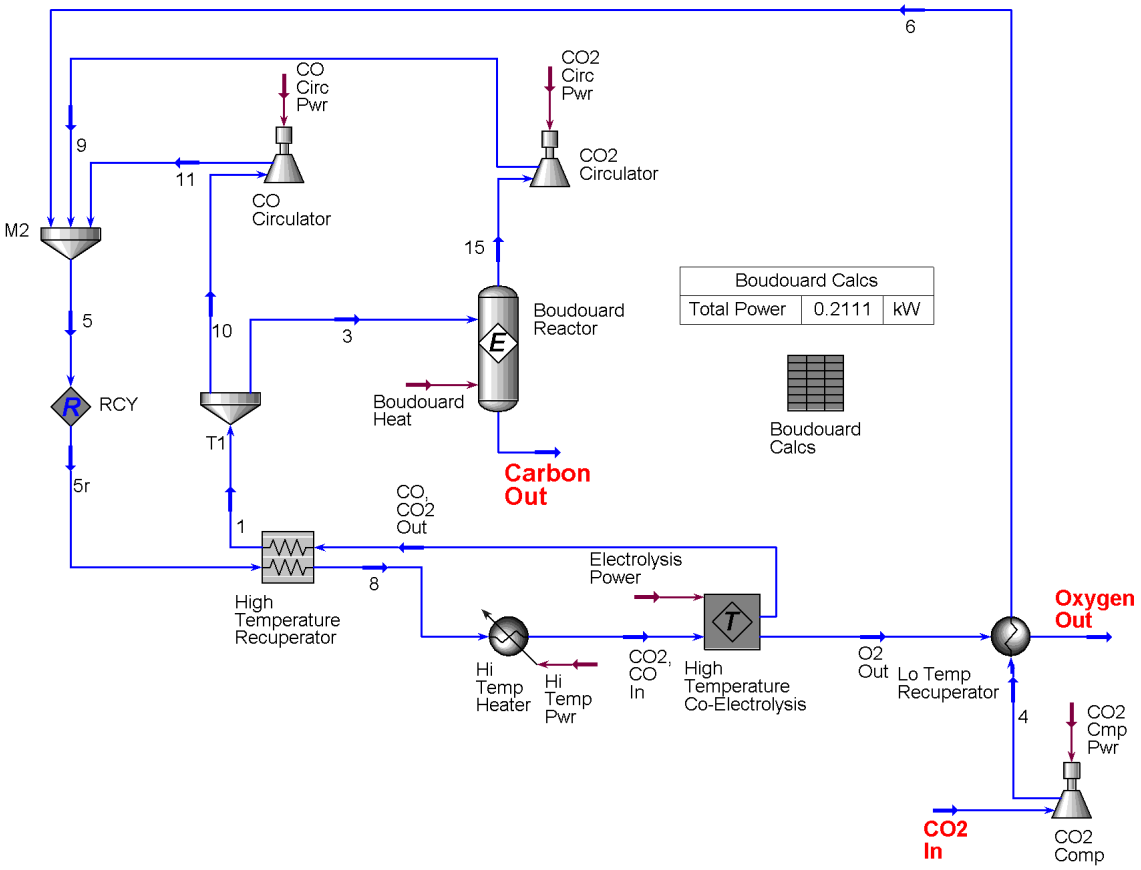

Figure 15. Process flow diagram of Boudouard process with co-electrolysis

This stream is mixed with carbon dioxide from the Boudouard reactor and some carbon monoxide from the co-electrolysis unit to constitute a molar flow of 10% carbon monoxide and 90% carbon dioxide. The carbon monoxide is used to provide reducing conditions at the carbon monoxide side of the solid oxide electrolysis cells. A high temperature recuperating heat exchanger heats the stream to nearly 700°C and is further heated to 800°C by an electric heater. The carbon dioxide is electrolyzed to carbon monoxide and oxygen in the electrolyzer. The molar composition of the exit stream at the carbon side of the electrolyzer is 90% carbon monoxide and 10% carbon dioxide. Electrolysis unit was set to avoid the full electrolysis of the carbon dioxide to prevent the formation of carbon within the electrolysis unit. If too much current is applied to the electrolysis cells, the carbon monoxide will reduce to form oxygen and solid carbon. The carbon could impair the cells. The carbon monoxide passes through the Boudouard reactor where solid carbon and carbon dioxide are formed at a temperature of 350°C. In this process no water or hydrogen is used and no methane is produced.

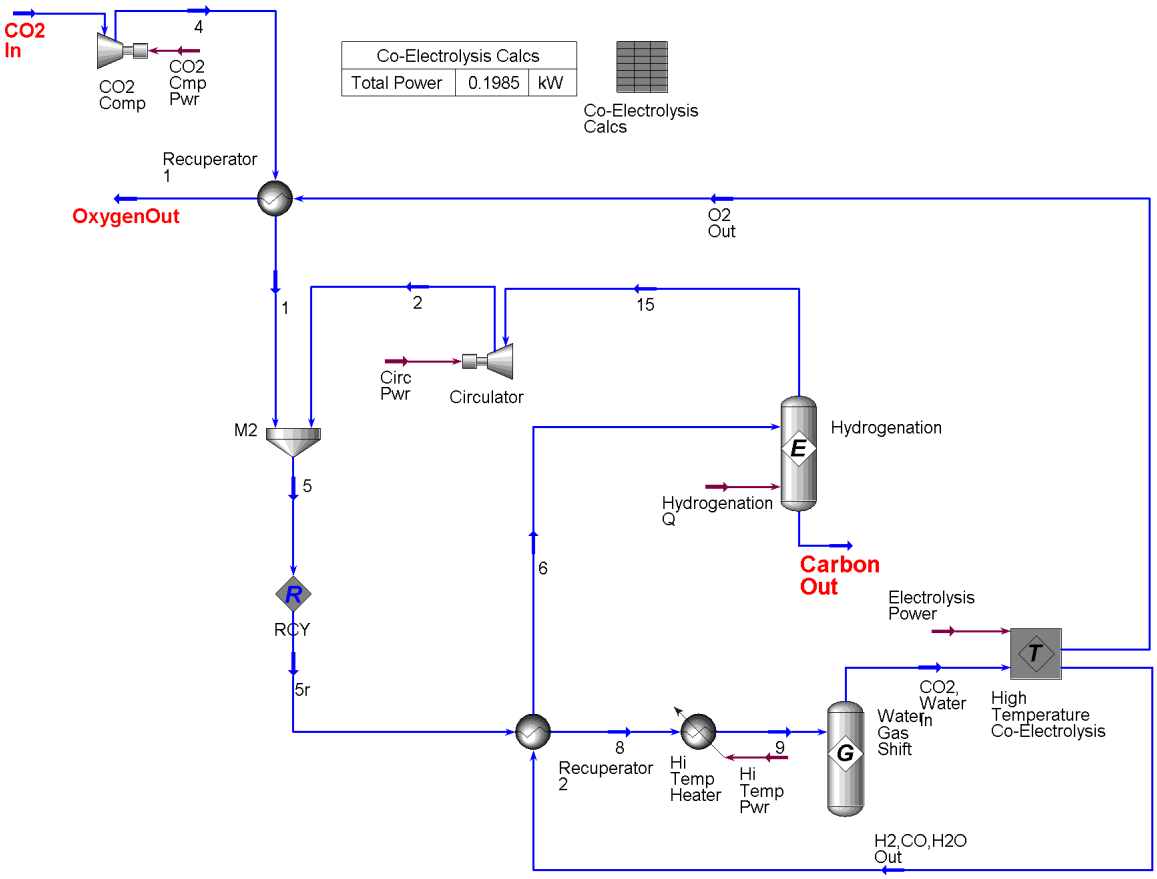

Figure 16. Process flow diagram of hydrogenation process with co-electrolysis

6. Hydrogenation and co-electrolysis integrated model

Hydrogenation is a process by which carbon monoxide and hydrogen are in equilibrium with water and carbon. Equilibrium data for the hydrogenation process were integrated into a HYSYS equilibrium reactor to simulate the process.

$$CO + H_2 \rightarrow H_2O + C \qquad (18)$$

The hydrogenation process was combined with high-temperature co-electrolysis to develop an alternative oxygen producing process as shown in Figure 16. Compressed carbon dioxide is heated using the hot oxygen stream exiting the co-electrolysis unit. The exit gas stream from the hydrogenation reactor, which is about 50% hydrogen and 40% steam by mole is mixed with the carbon dioxide and heated to over 700°C by the syngas and water mixture exiting the electrolysis unit. The gas is then heated to the electrolysis process temperature by an electric heater. Oxygen and a syngas stream are produced from the electrolysis unit. The syngas reacts in the hydrogenation reactor at a pressure of 172 kPa (25psia) and a temperature of 350°C to produce carbon and water. Ideally, the hydrogen and water within this overall process is recycled and therefore no need to replenish either.

V. Analysis of Process Models

7. Evaluation of models based on oxygen production at 1 kg/s

Table 1. Results for the production of 1 kg/s of oxygen

	CO_2 in (kg/day)	water in (kg/day)	total electric power (watts)
Bosch process with three compressors	1.310	0.033	212
Bosch process with at sub-atmospheric conditions	1.310	0.035	217
Bosch process with 1 compressor	1.310	0.040	244
Sabatier process	0.786	0.588	207
Co-electrolysis integrated Sabatier with recuperation	0.638	0.618	185
Co-electrolysis integrated Sabatier without heat recuperation	0.638	0.618	242
Co-electrolysis integrated Boudouard	1.375	0.000	211
Co-electrolysis integrated Hydrogenation	1.375	0.000	199

The scale of the process models was set at 1 kg/s of oxygen production to compare the processes. Table 1 shows the carbon dioxide and water inputs and the total power for oxygen production at I kg/ s. Tables 2 and 3 list the type and number of equipment required for each component with either power usage or duty needs. Table 2 is useful in estimating the overall system mass for each process.

The highest flow of CO_2 is associated with the co-electrolysis integrated Boudouard and Hydrogenation processes which also have no water input. The Bosch processes have slightly less CO_2 flows but require small amounts of water.

Table 2. Equipment for the production of 1 kg/s of oxygen, part 1

	compressors		pumps		heat exchangers		valves
	# of units	power (watts)	# of units	power (watts)	# of units	duty (watts)	# of units
Bosch process with three compressors	3	5.87	1	3.02E-06	1	317.3	1
Bosch process at sub-atmospheric conditions	1	10.3	2	6.72E-04	1	312.0	2
Bosch process with one compressor	1	37.4	1	3.38E-05	1	401.5	0
Sabatier process	1	0.23	2	2.96E-04	0	0.0	2
Co-electrolysis integrated Sabatier with recuperation	1	0.42	2	2.17E-04	3	59.7	2
Co-electrolysis integrated Sabatier without recuperation	1	0.32	1	1.94E-04	1	9.1	2
Co-electrolysis integrated Boudouard	3	0.79	0	0	2	18.4	0
Hydrogenation with Co-electrolysis	2	1.33	0	0	2	29.4	0

The lowest CO_2 flow rates are estimated for the Sabatier processes, with and without integrated co-electrolysis modules. They, however, have highest water flow rates. The CO_2 flow rate is affected by the rate of water coming into the system. Both ultimately produce oxygen and therefore as the water flow rate into the process increases, the carbon dioxide flow rate decreases.

When considering total electrical power into the process, the Bosch process with one compressor has the highest value at 244 watts. A comparison between the three-compressor and one-compressor cases shows a power reduction of nearly 15%, in favor of the three-compressor case. The separate compression of the hydrogen, carbon dioxide and recycle streams reduces the compression power from 28.6 watts to 4.48 watts. The Bosch process at sub-atmospheric conditions has a larger compression need than the three-compressor system, 10.3 watts compared to 5.87. However, the overall power usage is quite similar so that the advantage of one system over the other is inconclusive, based on this study. True pressure losses in both systems need to be determined. The co-electrolysis integrated Boudouard process compares well with Bosch process. The amount of power needed for the electrolysis processes are about the same. The Bosch process model used the thermodynamically less efficient low temperature electrolysis to electrolyze water. The Boudouard process model used a more efficient high-temperature electrolysis. However, it also electrolyzes CO_2, which requires more energy to split than water.

Table 3. Equipment for the production of 1 kg/s of oxygen, part 2

	condensers		reactors		electrolyzer	heaters	
	# of units	duty (watts)	# of units	duty (watts)	power (watts)	# of units	power (watts)
Bosch process with three compressors	1	-48.5	1	-16.6	207	0	0
Bosch process at sub-atmospheric conditions	1	-53.3	1	-15.9	207	0	0
Bosch Process with one compressor	1	-83.6	1	-13.3	206	0	0
Sabatier process	1	-15.3	1	-28.9	207	0	0
Co-electrolysis integrated Sabatier with recuperation	1	-16.1	1	-33.1	183	1	1.07
Co-ectrolysis integrated Sabatier without recuperation	1	-16.1	1	-51.7	183	2	58.2
Co-electrolysis integrated Boudouard	0	0	1	-66.4	205	1	5.60
Co-electrolysis integrated Hydrogenation	0	0	1	-54.2	192	1	5.40

The Sabatier process requires slightly less power than the Bosch processes due to lesser compression needs. The electrolysis power needs are the same. The co-electrolysis integrated Sabatier process has the least power requirement to produce oxygen at 1kg/s of due to the 11% reduction of power within the electrolysis unit. (Although an additional electric heater is needed to achieve electrolysis temperatures, the power increased only by one watt). However, to achieve this power reduction, nearly 60 watts of heat recuperation is necessary. If recuperation is not maintained, the overall power increases by 31%.

The co-electrolysis-integrated hydrogenation process has an overall power requirement that is the second lowest and the co-elctrolysis integrated Sabatier process has the lowest power demand. The electrolysis process has a lower power need than the co-electrolysis integrated Boudouard process because water is produced within the process and is the primary component that is electrolyzed. Water electrolyzes at a lower power than carbon dioxide because the heat of formation of water is lower. Estimated power numbers indicate that water electrolysis may be favored over CO_2 electrolysis when both carbon dioxide and water enter the co-electrolysis unit. As the water is depleted and hydrogen is produced, the hydrogen shifts the carbon dioxide to carbon monoxide and water. The new, shifted, water is then further electrolyzed. In the case of the co-electrolysis integrated Boudouard process, no water is

present and therefore the CO_2 is electrolyzed directly, resulting in a higher power usage. For hydrogenation process, water is created and therefore the power requirement of the electrolysis process is reduced.

The hydrogenation process requires heat recuperation to reduce power requirement. However, the recuperation duty is about half of that of the co-electrolysis integrated Sabatier process with heat recuperation. The power requirement for the hydrogenation process could have been further reduced if the heat from the hydrogenation reactor had been recuperated as well.

8. Evaluation of models based on CO_2 utilization at 1 kg/s

The data based on the models was adjusted so that the inlet flow of carbon dioxide was set to 1 kg/s. Results are shown in Tables 4, 5, and 6. Power usage is lower for the Bosch processes than for the Sabatier processes when the data was presented on the basis inlet flow of carbon dioxide (CO_2 utilization). Although more oxygen is produced in the Sabatier processes, more power is needed to electrolyze the incoming water as well as the water generated in the Sabatier reactor.

Table 4. Results for the processing of 1 kg/s of carbon dioxide

	O_2 out (kg/day)	water in (kg/day)	total electric power (watts)
Bosch process with three compressors	0.763	0.025	162
Bosch process with at sub-atmospheric conditions	0.763	0.027	165
Bosch process with one compressor	0.763	0.030	186
Sabatier process	1.272	0.748	263
Co-Electrolysis integrated Sabatier with recuperation	1.567	0.969	290
Co-electrolysis integrated Sabatier without recuperation	1.567	0.968	379
Co-electrolysis integrated Boudouard	0.727	0.000	153
rolytegrated Hydrogenation	0.727	0.000	144

Table 5. Equipment for the processing of 1 kg/s of carbon dioxide, part 1

	compressors		pumps		heat exchangers		valves
	# of units	power (watts)	# of units	power (watts)	# of units	duty (watts)	# of units
Bosch process with three compressors	3	4.48	1	2.31E-06	1	242.2	1
Bosch pocess at sub-atmospheric conditions	1	7.83	2	5.13E-04	1	238.2	2
Bosch process with one compressor	1	28.56	1	2.58E-05	1	306.5	0
Sabatier process	1	0.29	2	3.77E-04	0	0.0	2
Co-electrolysis integrated Sabatier with recuperation	1	0.67	2	3.40E-04	3	93.5	2
Co-electrolysis integrated Sabatier without recuperation	1	0.50	1	3.03E-04	1	14.3	2
Co-electrolysis integrated Boudouard	3	0.58	0	0.00E+00	2	13.4	0
Co-electrolysis integrated Hydrogenation	2	0.96	0	0.00E+00	2	21.4	0

Most of the water for the Bosch processes comes from carbon dioxide as it is processed through the Bosch reactor. The co-electrolysis integrated Boudouard and hydrogenation processes have the lowest power usage to process 1 kg/s of carbon dioxide. However, they also have the lowest oxygen production. Both of these processes have no incoming water.

Table 6. Equipment for the processing of 1 kg/s of carbon dioxide, part 2

	condensers		reactors		electrolyzer	heaters	
	# of units	duty (watts)	# of units	duty (watts)	power (watts)	# of units	power (watts)
Bosch process with three compressors	1	-37.0	1	-12.7	158	0	0
Bosch process at sub-atmospheric conditions	1	-40.7	1	-12.1	158	0	0
Bosch process with one compressor	1	-63.8	1	-10.1	158	0	0
Sabatier process	1	-19.5	1	-36.8	263	0	0
Co-electrolysis integrated Sabatier with recuperation	1	-25.3	1	-51.8	287	1	1.68
Co-electrolysis integrated Sabatier without recuperation	1	-25.3	1	-81.1	287	2	91.27
Co-electrolysis integrated Boudouard	0	0.0	1	-48.3	149	1	4.07
Co-electrolysis integrated Hydrogenation	0	0.0	1	-39.4	139	1	3.92

The Boudouard process requires more power because carbon dioxide is electrolyzed directly in the electrolysis unit. The hydrogenation reactor produces water that passes through the electrolysis unit with the carbon dioxide. Compression power requirements are low for all the Sabatier processes as well as the Boudouard and hydrogenation processes.

Heat exchanger duties are highest with the Bosch processes due to the higher temperatures within the reactors. The co-electrolysis integrated Boudouard and hydrogenation processes have no condensers. It is interesting to note that the co-electrolysis integrated Sabatier process requires more power than the base Sabatier process to convert 1kg/s of carbon dioxide, because the water requirement is higher.

Carbon Balance

A carbon balance was performed to determine where the carbon goes with each process. A constant oxygen production and a constant carbon dioxide processing analysis were performed and the results are listed in Tables 7 and 8.

For the Bosch processes and the co-electrolysis integrated Boudouard and hydrogenation processes, the carbon exits as a solid. With the Sabatier processes, carbon exits the reactor, primarily as methane. The Sabatier with default electrolysis has also some carbon exit as carbon dioxide.

When the inlet with the outlet mole balances are compared, all cases balance well except the Bosch. Some water was added to these cases to produce additional hydrogen for the Bosch processes. However, a means to remove the hydrogen after the process was not provided which cause an unbalanced mass inventory. The water flow in for these cases was small and therefore difference is mass is small. When looking at the case with constant carbon dioxide flow, the difference is more pronounced.

Table 7. Carbon balance for producing 1 kg/s of oxygen

carbon in (gmole/hr)	carbon out (gmole/hr)					carbon out %			
CO_2	C	CO	CO_2	CH_4	Total	C	CO	CO_2	CH_4
1.24	1.22				1.22	100%	0%	0%	0%
1.24	1.25				1.25	100%	0%	0%	0%
1.24	1.22				1.22	100%	0%	0%	0%
0.744		2.34E-07	9.45E-02	0.650	0.744	0%	0%	13%	87%
0.604		5.64E-12	6.40E-08	0.604	0.604	0%	0%	0%	100%
0.604		5.59E-12	6.33E-08	0.604	0.604	0%	0%	0%	100%
1.30	1.30				1.30	100%	0%	0%	0%
1.30	1.30				1.30	100%	0%	0%	0%

Table 8. Carbon balance for processing 1 kg/s of carbon dioxide

carbon in (gmole/hr)	carbon out (gmole/hr)					carbon out %			
CO_2	C	CO	CO_2	CH_4	Total	C	CO	CO_2	CH_4
0.947	0.932	0.000	0.000	0.000	0.932	100%	0%	0%	0%
0.947	0.952	0.000	0.000	0.000	0.952	100%	0%	0%	0%
0.947	0.933	0.000	0.000	0.000	0.933	100%	0%	0%	0%
0.947	0.000	0.000	0.120	0.827	0.947	0%	0%	13%	87%
0.947	0.000	0.000	0.000	0.947	0.947	0%	0%	0%	100%
0.947	0.000	0.000	0.000	0.947	0.947	0%	0%	0%	100%
0.947	0.947	0.000	0.000	0.000	0.947	100%	0%	0%	0%
0.947	0.947	0.000	0.000	0.000	0.947	100%	0%	0%	0%

VI. Conclusions and Recommendations

If water is added to one of the processes, the power to produce oxygen goes down per unit mass of oxygen but less carbon dioxide is processed since the energy of formation for water is less than that for carbon dioxide. From the perspective of the reduction of mass and energy consumption, addition of water leads to additional mass load of the water.

High temperature co-electrolysis is thermodynamically more efficient than low temperature electrolysis. However, a means is needed to raise the temperature of the carbon dioxide and water to the electrolysis temperature of 800°C. Based on these factors, the following conclusions may be derived from this study.

- The Bosch processes have higher power requirements when considering oxygen production alone, but it offers higher carbon dioxide conversion per unit power input, compared to other processes studied.
- The Sabatier processes require lower power when considering oxygen production alone, but require more water input, compared to other processes studied.
- For pure oxygen production, the co-electrolysis integrated Sabatier process requires the least amount of power among the processes studied. However, it also has the highest water requirement. Per unit mass of CO_2 utilized, this process, however, has the highest power requirement.
- The co-electrolysis integrated Boudouard process agrees well with the base Bosch process when considering oxygen production, but processes carbon dioxide with comparatively less power.

- Co-electrolysis integrated hydrogenation process has the best overall performance. For pure oxygen production, it is the second best (with the co-electrolysis integrated Sabatier process being the best) in terms of power requirement. However, it performs better than all of the processes in terms of carbon dioxide utilization.
- If co-electrolysis is used, heat recuperation is necessary to reduce power consumption.

The following recommendations should be considered for further study:

- The Bosch processes need to be modeled without any water input to be consistent with other models to make the carbon inflow more in balance with the carbon outflow.
- If a small amount of water is desired for the Bosch process, a hydrogen purge stream needs to be added to improve the mass balance.
- The models for this study have assumed steady state operation and chemical equilibrium within the reactors. The kinetics of the reactors need to be considered to model more realistic chemical reactions.

VII. Discussion on Degradation Possibilities of SOEC [9]

Thermal cycling due to shutdown and startup operations and thermal gradients on electrochemical reaction sites due to uneven heat distribution can cause large thermal stresses and potential failure of the cell. Existing degradation data can be classified as (a) baseline progressive constant-rate degradation, (b) degradation corresponding to transients caused by thermal or redox (**red**uction and **ox**idation) cycling phenomena occurring in a cell, and (c) degradation resulting from a sudden incident or a failure/malfunction of a component or a control in a stack system. However, there is no clear evidence if different events lead to similar or drastically different electrochemical degradation mechanisms within a cell.

Main sources of degradation come from several cell components. Details about the following list of general observations and main sources of SOEC stack degradation have been discussed in earlier sections:

- Delamination of O_2-electrode side bond layer from the O_2-electrode
- Bond layer on steam/H_2-electrode side is not degrading
- Air and steam/H_2 flow fields (flow channels) are not degrading
- Five cell components are suspect
    - Bond layer on O_2-electrode-Cr poisoning and dissociation
    - O_2-electrode-microstructural changes and delamination
    - Loss of electrical/ionic conductivity of electrolyte
    - Interconnect-generation of contaminants
    - Steam/H_2- electrode

The degradation mechanisms in a stack are not identical to that in a single cell. Also, degradation in a SOEC is not identical to that in a SOFC. Long-term, single-cell tests show that SOEC operation has greater degradation rates than that in SOFC mode.

It is understood that degradation of the O_2-electrode is more severe than that of the H_2-electrode. ANL examination of a SOEC operated by INL for ~1,500 hours showed that O_2-electrode delaminated from the bond layer/electrolyte. In SOEC mode, O_2 has to be pushed out, hence chances of delamination increase. Therefore, the high porosity of O_2-electrode is very important. Per ANL observations, the delamination occurs in cell areas with high current flows. It has also been suggested that chromium poisoning originating from the interconnects or the balance-of-plant pipes may get located at the interface or triple phase boundary (TPB). This can result in bond layer getting separated from the O_2-electrode. Deposition of impurities at the TPB and delamination can adversely impact the electrochemical reactions and ionic conductivity in the cell.

In electrolytes, the main cause of degradation is loss of electrical/ionic conductivity. Müller et al. [10]showed that during first 1,000 hours of testing, yttria and scandia doped zirconia (8 mol% Y_2O_3 $ScZrO_2$/8YSZ) electrolytes showed ~23% of degradation. For the next 1,700 hours of testing, the decrease in conductivity was as high as 38%.

Overall, many researchers agree that the contribution of a steam/H_2-electrode to SOEC degradation is much less than that of other cell components. ANL also observed Si as a capping layer on steam/H_2-electrode. It probably was carried by steam from the seals, which contain Si. SiO_x also emanates from interconnect plates. In literature, it has

been noted that steam content greater than 30% shows conductivity loss. Therefore, an optimum ratio of steam-H_2 mixture and steam utilization percentage needs to be determined.

Interconnects can be a source of serious degradation. Sr, Ti, and Si segregate and build-up at interfaces. Sr segregates to the interconnect–bond layer interface. Mn segregates to the interconnect surface. Si and Ti segregate to the interconnect-passivation layer interface. Cr contamination can originate from interconnects and it can interact with O_2-electrode surface or even diffuse into the O_2-electrode. Coated stainless steel interconnects have shown reduced degradation rates. GE observed higher degradation with stainless steel current collectors than with Au current collectors [7]

A hydrogen electrolysis plant or a laboratory-scale experiment is always connected to the pipes, gas storage tanks/cylinders, or other such equipment. These components can be a source of undesirable particles/chemicals, which can get deposited at different locations in a solid oxide electrolysis cells. It has been shown in previous sections that any foreign particles depositing at the triple phase boundary can lead to degradation in cell performance. The reactant gases can also have some undesirable impurities. It is understood that the balance of plant and gases are merely sources of impurities. The phenomenological causes of degradation depend on other electrochemical reasons.

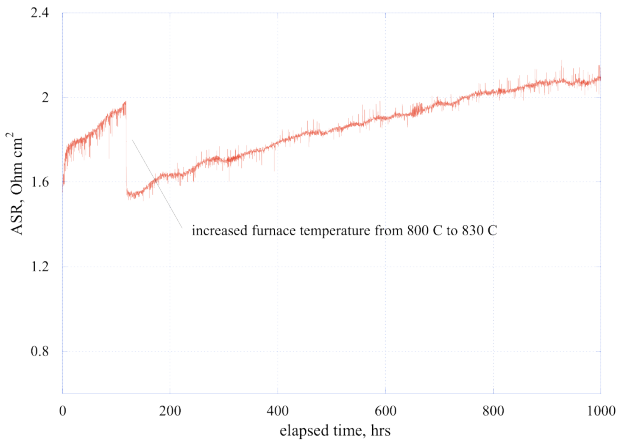

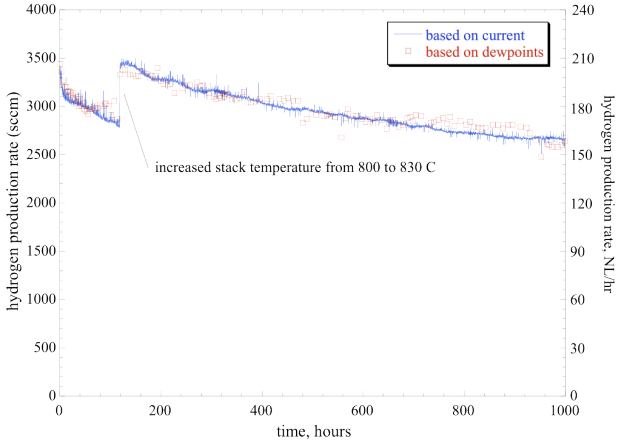

Figure 17.

Figure 18.

ASR of a 25-cell stack as a function of time for a 1,000-hour (Figure 17) H_2 production rate during 1,000 hour and co-electrolysis (Figure 18) processes

the glass seals were replaced. Nickel from nickel mesh can volatize in high water content environments, move into the steel and make it austenitic, which will eventually corrode. Silica poisoning is a potential problem. Impure water can contain Si. Therefore, in SOEC, it is likely that high temperature steam interacting with balance-of-plant piping picks up Si and transports it elsewhere to form nonconductive scale. Iron can also diffuse into glass seals and cause electrical shorting. Mn diffuses from interconnect, but its effect on degradation is unknown. Phosphorus and arsenic can react and interact with the electrode containing Ni. They can form eutectics and enhance Ni mobility. This is a very low-level effect.

Performance degradation results with a 25-cell SOEC stack tested for 1,000 hours at INL are shown in Figures 19 and 20. [11] Figure 19 plots the stack ASR as a function of time for the 1,000 hours. The furnace temperature was increased from 800 to 830°C over an elapsed time of 118 hours, resulting in a sudden drop in ASR. The increase in ASR with time represents degradation in stack performance. The degradation rate decreases with time and is relatively low for the last 200 hours of the test. However, from the 118-hour mark to the end of the test, the ASR increased more than 40% over approximately 900 hours. Reduction of this performance degradation is an objective of ongoing research. Figure 4 shows the corresponding generation of hydrogen.

References

1. [1] Mulloth L. M., Rosen M., Affleck D. L., Varghese M., LeVan D. M., Moate J. R., Knox J. C., (2005). "Development of a Low-Power CO_2 Removal and Compression System for Closed-Loop Air Revitalization in Future Spacecraft", SAE, Paper No> 2005-01-2944, International Conference on Environmental Systems.

2. [2] Genovese J., "Impact of CO_2 Reduction Technology Choice on a Closed System Water Balance", (2003). SAE, Paper No. 1999-01-2120, International Conference on Environmental Systems

3. [3] Murdoch, K. E., Allen, G.F. Jr., (1999). "Parametric Impacts on Sabatier Water Production Capability", SAE Paper No. 1999-01-2121, International Conference on Environmental Systems

4. [4] Murdoch, K.E., Perry, J.L., Smith, F.D., (2003). "Sabatier Engineering Development Unit", SAE, Paper No. 2003-01-2496, International Conference on Environmental Systems.

5. [5] Holmes, R. F., Keller, E. E., Kilzg, C. D., (1970). "A Carbon Dioxide Reduction Unit Using Bosch Reaction and Expendable Catalyst Cartridges" NASA Report, CONVAIR Division of General Dynamics Corporation San Diego, California.

6. [6] Stoots, C. M., O'Brien, J. E., Hawkes, G. L., Herring J. S., Hartvigsen, J. J., (2006). "High Temperature Co-Electrolysis of H_2O and CO_2 for Syngas Production," Paper No. 418, Fuel Cell Seminar.

7. [7] Guan, J. et al. (2006). "High Performance Flexible Reversible Solid Oxide Fuel Cell," GE Global Research Center Final Report for DOE Cooperative Agreement DE-FC36-04GO-14351.

8. [8] Gazzari, J. I., Kesler, O., (2007). "Non-destructive Delamination Detection in Solid Oxide Fuel Cells," J. Power Sources, Vol. 167, pp. 430-441.

9. [9] Sohal, M. S. et al. (2009b). "Critical Causes of Degradation in Integrated Laboratory Scale Cells during High Temperature Electrolysis," INL Report INL/EXT-09-16004.

10. [10] Müller, A.C., Weber, A., Herbstritt, D., and Ivers-Tiffée, E. (2003). "Long Term Stability of Yttria and Scandia doped Zirconia Electrolytes," Proceedings 8th International Symposium on SOFC, (Edited by) Singhal, S. C., Dokiya, M., PV 2003-07, The Electrochemical Society, 196-199.

11. [11] O'Brien, J. E., Stoots, C. M., Herring, J. S., and Hartvigsen, J. J. (2007). "Performance of Planar High-Temperature Electrolysis Stacks for Hydrogen Production from Nuclear Energy," Nuclear Technology, 158, 118-131.